



Article

# Assessing the Effect of Fe<sub>3</sub>O<sub>4</sub> Nanoparticles on the Thermomechanical Performance of Different Forms of Carbon Allotropes/Epoxy Hybrid Nanocomposites

Sotirios G. Stavropoulos , Aikaterini Sanida and Georgios C. Psarras \*

Smart Materials & Nanodielectrics Laboratory, Department of Materials Science, School of Natural Sciences, University of Patras, 26504 Patras, Greece; stavropoulos@upatras.gr (S.G.S.); ksanida@upatras.gr (A.S.)

\* Correspondence: g.c.psarras@upatras.gr; Tel.: +30-2610-996-316

**Abstract:** The incorporation of ceramic nanoinclusions in carbon nanocomposites can induce additional functionality in the field of magnetic properties, piezoelectricity, etc. In this study, series of nanocomposites, consisting of different carbon nanoinclusions (carbon black, MWCNTs, graphene nanoplatelets, nanodiamonds) and magnetite nanoparticles incorporated into a commercially available epoxy resin were developed varying the filler type and concentration. Experimental data from the static tensile tests and dynamic mechanical analysis (DMA) demonstrated that the elastic tensile modulus and storage modulus of hybrid nanocomposites increase with an increase in filler content up to almost 100% due to the inherent filler properties and the strong interactions at the interface between the epoxy matrix and the nanoinclusions. Strong interactions are implied by the increasing values of the glass transition temperature recorded by differential scanning calorimetry (DSC). On the contrary, tensile strength and fracture strain of the nanocomposites were found to decrease with filler content. The results highlight the potentials and capabilities of developing hybrid multifunctional nanocomposites with enriched properties while holding their structural integrity.

**Keywords:** polymer nanocomposites; magnetite; carbon black; carbon nanotubes; graphene nanoplatelets; nanodiamonds; thermomechanical properties; elastic modulus; tensile strength



**Citation:** Stavropoulos, S.G.; Sanida, A.; Psarras, G.C. Assessing the Effect of Fe<sub>3</sub>O<sub>4</sub> Nanoparticles on the Thermomechanical Performance of Different Forms of Carbon Allotropes/Epoxy Hybrid Nanocomposites. *Appl. Mech.* **2022**, *3*, 560–572. <https://doi.org/10.3390/applmech3020033>

Received: 23 March 2022

Accepted: 4 May 2022

Published: 6 May 2022

**Publisher's Note:** MDPI stays neutral with regard to jurisdictional claims in published maps and institutional affiliations.



**Copyright:** © 2022 by the authors. Licensee MDPI, Basel, Switzerland. This article is an open access article distributed under the terms and conditions of the Creative Commons Attribution (CC BY) license (<https://creativecommons.org/licenses/by/4.0/>).

## 1. Introduction

The ongoing need for lightweight and strong materials that exhibit new fascinating properties with enhanced and more versatile performance than the conventional monolithic engineering materials has paved the way to the introduction of advanced composite materials. Among such composite materials, polymer-based composites have attracted the interest of materials' scientists and engineers because of their deep-rooted advantages that include high strength to weight ratio, ease processing and forming, thermomechanical stability, high dielectric breakdown strength and low cost [1–3].

Besides the well-established enhancement of the mechanical performance of polymer nanocomposites, the addition of suitable reinforcing agents can considerably modify the behavior at service of the polymer matrix inducing tailored electric, magnetic and other functional properties [4–8]. The simultaneous incorporation of multiple functional constituents combining different desirable properties into a polymer matrix makes possible the design and development of novel hybrid multifunctional composite materials with the versatility to respond to different conditions, thus being able to perform the operations of sensing, actuation and energy storage/harvesting [9,10].

Epoxy resin has been widely adopted as a matrix material for the fabrication of advanced technological composites used in automobile, aerospace, electronics, wind energy and civil applications due to epoxy resin's outstanding characteristics including good adhesion to fiber reinforcements, compatibility with various curing systems, thermal, mechanical, electrical and chemical properties [11–14].

Carbon is arguably the most investigated material as reinforcement in polymer composites since the development of carbon fibers more than 50 years ago, with an abundance of applications at the industrial level [2,15]. The introduction of nanoscaled forms of carbon allotropes with versatile spatial configurations and dimensionality such as carbon nanotubes, graphene or carbon black promised exotic mechanical properties of the order of TPa, although a limited percentage of this performance has been translated into carbon reinforced polymer nanocomposites [11,12,16–18]. Nevertheless, the unique properties exhibited by polymer nanocomposites filled with carbonaceous nanoparticles of various allotropes are driving the research in a vast range of potential applications [19].

$\text{Fe}_3\text{O}_4$ , a name synonymous with magnetic response since antiquity, is a transition metal oxide exhibiting an inverse cubic spinel structure. Magnetite is used in a wide-ranging area of applications such as telecommunications, data storage, magnetic inks, microwave-based devices, high-frequency electronics, magnetic recording technology and electrical energy production and supply [20,21].

While there are many studies showcasing the advantages of hybrid polymer nanocomposites, several challenges need to be resolved before the industrial sector can follow with the mass production of such systems. In order to produce these advanced composite materials, engineers have to ensure the homogeneous dispersion of nanofillers in the epoxy matrix coupled with strong interfacial bonding between the nanoinclusions and the macromolecules. Chemical functionalization techniques have been employed to enhance the chemical compatibility between the fillers trying to improve the overall properties of hybrid epoxy nanocomposites [16,22]. However, the disparity between the different designs and employed procedures makes difficult the direct comparison and commercial exploitation of experimental results presented in the literature. Further challenges including some non-desirable properties in the composites derived from the functionalization processes and the dimensional discrepancy between the two types of filler pose additional obstacles to scale up the production [13,23].

For this reason, in this study commercially available reagents were used in order to assess the effect of the different employed nanoparticles on the final properties of fabricated systems that would be low-cost and easy to produce in a mass industrial scale. Series of hybrid carbon allotropes (carbon black, multi-walled carbon nanotubes, graphene nanoplatelets and nanodiamonds)/ $\text{Fe}_3\text{O}_4$ /epoxy nanocomposites were fabricated using an identical procedure with varying amounts of filler contents and their thermomechanical performance and structural integrity were evaluated via differential scanning calorimetry, static tensile tests and dynamic mechanical analysis.

## 2. Materials and Methods

### 2.1. Materials

Series of hybrid polymer nanocomposites were developed varying the filler type and content. A two-component low viscosity epoxy resin was employed as matrix, consisting of the epoxy prepolymer (diglycidyl ether of bisphenol A (DGEBA)) and an aromatic amine serving as the curing agent. The commercially available epoxy resin, namely Epoxol 2004, was provided by Neotex S.A., Athens Greece.

All fabricated systems had one filler in common, in particular iron oxide (magnetite  $\text{Fe}_3\text{O}_4$ ) nanoparticles with mean diameter less than 100nm supplied by Sigma Aldrich, Saint Louis, MO, USA.

A different type of carbon allotrope was acting as the secondary filler in each nanocomposite series. Namely,

(a) carbon black (CB) nanoparticles with a mean diameter of 13 nm and a specific surface area of approximately  $550 \text{ m}^2/\text{g}$ ,

(b) graphene nanoplatelets (GnP) with a thickness of 1–4 nm, particles' lateral size up to  $2 \mu\text{m}$  and specific surface area of  $700\text{--}800 \text{ m}^2/\text{g}$ ,

(c) multi-walled carbon nanotubes (MWCNT) (3–15 walls) with a length of 1–10  $\mu\text{m}$ , inner diameter 2–6 nm, outer diameter 5–20 nm and specific surface area  $240 \text{ m}^2/\text{g}$ ,

(d) nanodiamonds grade G (ND), with an average particle size of 4 nm and a specific surface area approximately 290–360 m<sup>2</sup>/g.

All carbon allotropes were supplied by Plasmachem GmbH.

## 2.2. Fabrication Procedure

For each nanocomposite series, a pre-calculated amount of carbon nanoparticles was mixed with the epoxy prepolymer by stirring at ambient temperature inside a sonicator for 10 min. Subsequently, the curing agent was added in the mixture at a 2:1 *w/w* mixing ratio of the epoxy prepolymer and the curing agent followed by additional stirring in the sonicator for another 5 min. Next, the magnetite nanoparticles were also added in the mixture and the final stirring in the sonicator took place for another 5 min. Upon completion of the previous step, the mixture was poured into suitable silicon molds to be cured for 7 days, at ambient temperature. Finally, all systems underwent a post curing procedure for 4 h at 100 °C. A schematic illustrating the steps of the fabrication process is depicted in Figure 1. Filler concentration for all systems was the combination of 0, 1, 10, 20 parts per hundred resin per weight (phr) magnetite nanoparticles with 0, 1, 3, 5, 10 phr of each allotropic form of carbon.

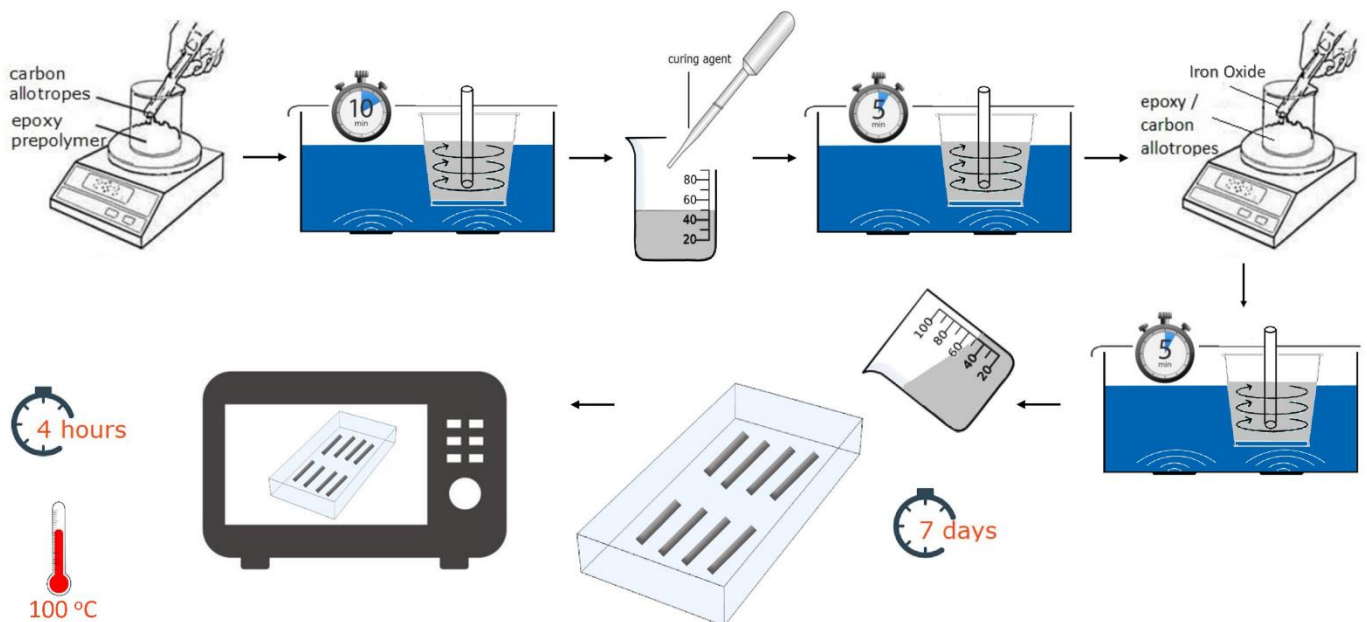


**Figure 1.** Schematic representation of the fabrication process of the nanocomposites.

## 2.3. Characterization Techniques

The morphology of the prepared nanocomposites as well as the state of the dispersion and distribution of particles in the epoxy matrix was examined by means of scanning electron microscopy (SEM) using a Carl Zeiss EVO MA 10 apparatus.

The thermal properties of the systems were investigated in the temperature range from 20 to 100 °C with a heating of 5 °C/min. by employing differential scanning calorimetry (DSC) using a TA Q200 device apparatus provided by TA Instruments. Samples were placed into an aluminum crucible with an empty crucible acting as reference.

The thermomechanical characterization was conducted by dynamic mechanical analysis (DMA) from room temperature to 100 °C, with a temperature rate of 5 °C/min and frequency of 1 Hz, using DMA Q800 by TA Instruments, in the 3-point bending configuration.

The mechanical response of the systems under tensile stress was examined by performing static tensile test, at ambient temperature and at 5 mm/min tension rate, using an Instron 5582 universal tester.

### 3. Results and Discussion

#### 3.1. Morphology

In order to obtain a clear picture of the nanoparticles' distribution and dispersion inside the polymer matrix, several SEM images were taken at various magnifications. Representative images for all examined systems are depicted in Figure 2. The morphological characterization verified the successful fabrication of the nanocomposites. The quality of the systems is deemed to be satisfactory as there was no detection of either cracks or encapsulation of air bubbles inside the material. In general, nanoinclusions were homogeneously distributed into the polymer matrix, nanodispersion was achieved and no severe agglomeration was detected. In systems with high filler content (especially carbon nanoparticles), a limited number of aggregates was present and a scarce number of carbon-rich or magnetite-rich domains were formed.

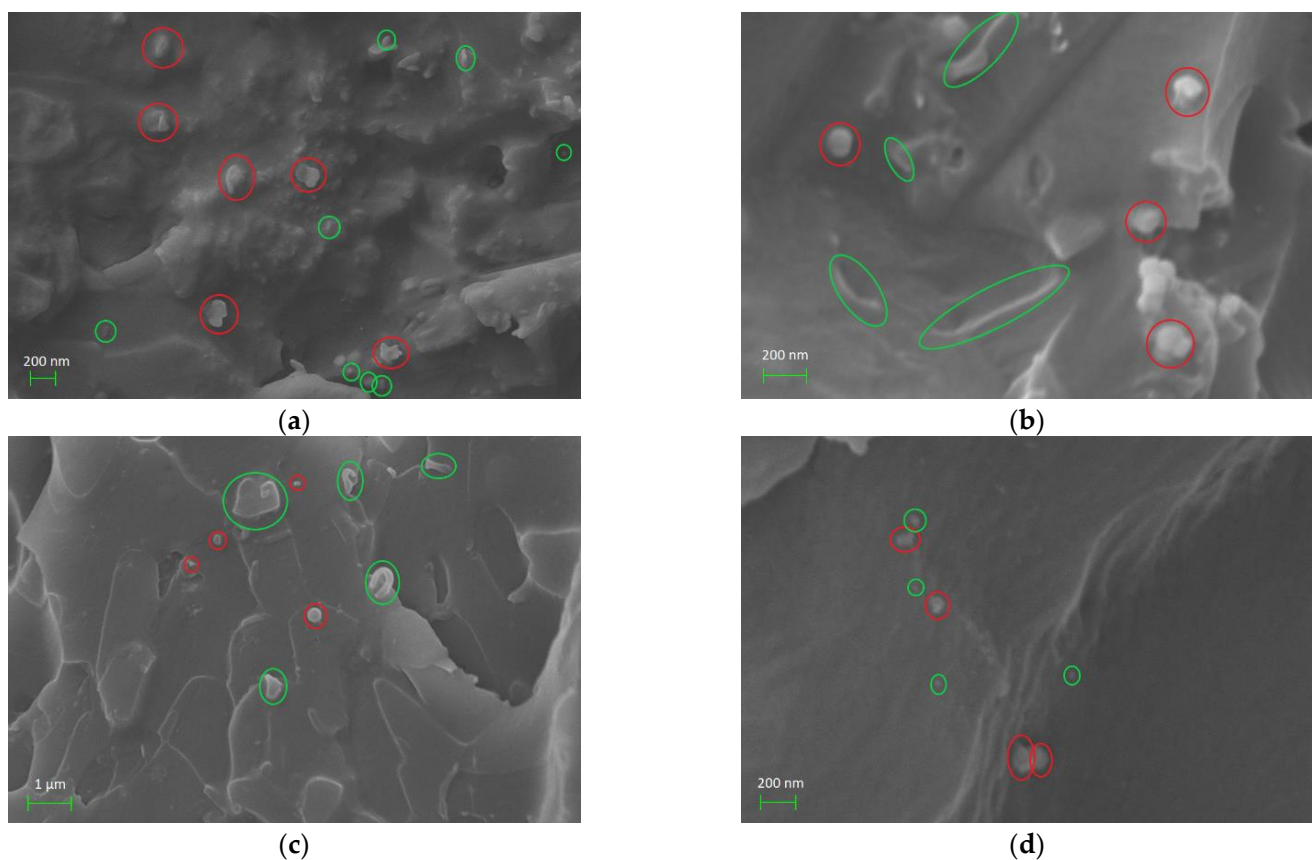


**Figure 2.** SEM images of the fabricated nanocomposites with 10 phr  $\text{Fe}_3\text{O}_4$  and 5 phr (a) CB; (b) MWCNT; (c) GnP; (d) ND concentration. Green circles denote the respective type of the carbon allotrope, while red circles indicate the  $\text{Fe}_3\text{O}_4$  nanoparticles.

#### 3.2. Differential Scanning Calorimetry

The thermal properties of the nanocomposites were investigated by employing differential scanning calorimetry. An endothermic step-like process was recorded in the thermograms of all examined systems that was related to the transition from the glassy rigid state to the rubbery state of the polymer matrix. Figure S1 displays a thermogram representative of the thermal behavior of all examined systems. The characteristic glass transition temperature for all nanocomposites was determined at the point of inflection using appropriate software provided by TA instruments. The results are depicted in Figure 3.

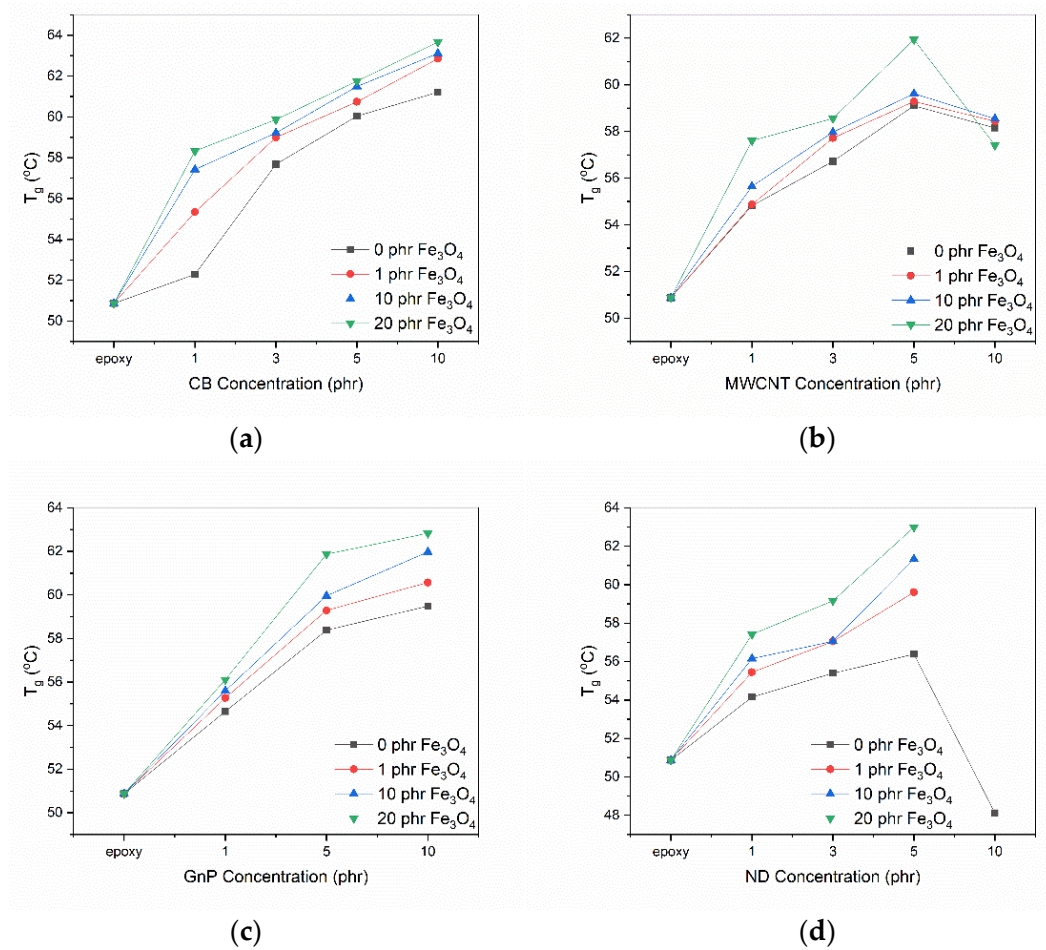


**Figure 3.** Glass transition temperature as a function of (a) CB; (b) MWCNT; (c) GnP; (d) ND concentration for all examined systems.

The variation of the glass transition temperature with filler content can be used to investigate the different interactions occurring inside the materials. The substantial increase of  $T_g$  values is the consequence of the obstruction of the cooperative segmental movement of the polymer chains imposed by the strong interactions between the nano-inclusions and the macromolecules. The higher glass transition temperature values than the neat epoxy exhibited by all hybrid nanocomposites imply good adhesion of the reinforcing phase to the polymeric matrix. The addition of carbon nanoparticles delivers a progressive increase in  $T_g$  values with filler content. On the other hand, even though glass transition temperature increases further with the addition of magnetite nanoparticles, its effect appears to be less pronounced compared to the nanocarbonaceous influence, with the exception of the nanocomposites filled with nanodiamonds. At high concentrations for the MWCNT filled nanocomposites, the stronger interactions between neighboring nanoparticles, on account of their aspect ratio, offset portion of the obstruction of the chain mobility, decreasing to some extent the values of the glass transition temperature. The substantial drop in the  $T_g$  value for the nanocomposite with 10 phr nanodiamond content, along with its respective mechanical performance, showed that there was no reason for the fabrication of hybrid nanocomposites with 10 phr nanodiamond content.

### 3.3. Dynamic Mechanical Analysis

The viscoelastic properties of the examined systems were investigated via dynamic mechanical analysis in the three-point bending configuration. Storage modulus takes its maximum value at low temperatures where the polymer matrix is in the rigid glassy state. An abrupt decrease in the storage modulus values with increasing temperature signals the glass to rubber transition of the polymer matrix, where the systems lose their load bearing capabilities. These transitions are identified by the formation of peaks in the loss modulus diagrams. This behavior, representative for all examined systems, is illustrated in Figure S2. Figure 4 depicts the variation of the maximum value of flexural storage modulus as a function of filler content.

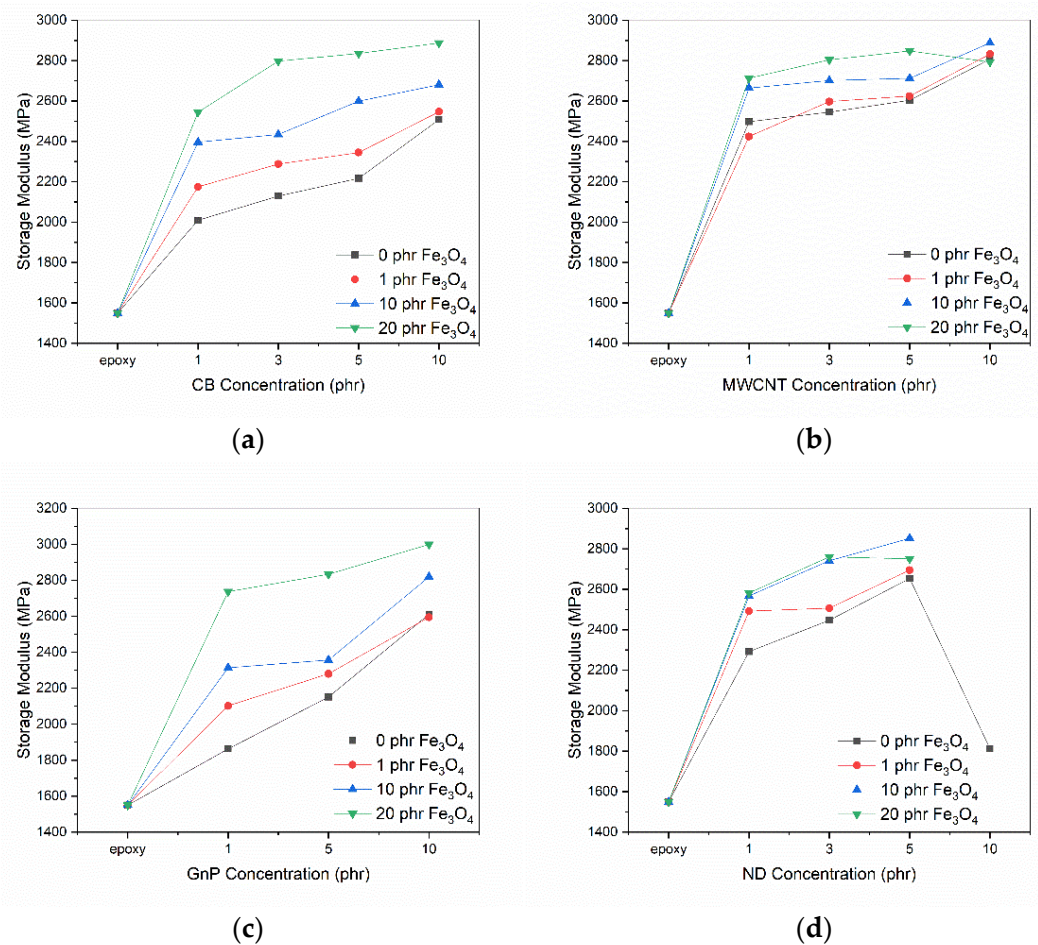


**Figure 4.** Storage modulus as a function of (a) CB; (b) MWCNT; (c) GnP; (d) ND concentration for all examined systems.

Storage modulus increases, in general, with the addition of both types of reinforcing nanoparticles reaching up to 3 GPa for the nanocomposite with 10 phr GnP and 20 phr iron oxide content, an almost 90% growth compared to the neat epoxy. The interactions between the added ceramic nanoparticles and the 2D carbon allotropes presumably lead to the reorganization of the filler arrangement inside the polymer matrix and the formation of a robust network that is able to effectively distribute the exerted mechanical stress. However, the excessive incorporation of the ceramic reinforcements in the polymer matrix leads to a slight decline in the storage modulus of the systems filled with the maximum concentration of MWCNT and nanodiamonds. At the lowest concentration of magnetite nanoparticles, the increase in the storage modulus values varies between 10% for the MWCNT filled systems to 48% for the GnP filled nanocomposites. The addition of magnetite nanoparticles has a more prominent effect in the systems filled with low content of

carbon allotropes, while the impact of the addition of  $\text{Fe}_3\text{O}_4$  nanoparticles varies between the systems with different carbon nano-inclusions with increasing nanocarbon content. The synergistic effect between the different types of filler is demonstrated with significantly enhanced thermomechanical response for the GnP and carbon black systems. On the other hand, the influence of magnetite nanoparticles' addition tends to be less significant for the MWCNT and nanodiamonds filled systems, becoming almost negligible with high ceramic filler loading. Overall, it can be assumed that, despite the reinforcing ability of the nano-inclusions, all systems reach a point, a kind of limit imposed by the polymer matrix and its synergy with the filler, where the additional filler content does not lead to further significant enhancement of the thermomechanical properties of the nanocomposites, as implied by the proximity of the maximum storage modulus values for all examined series.

### 3.4. Static Tensile Tests

The mechanical properties of polymer nanocomposites are determined by numerous parameters that include the particular properties of the components, the filler aspect ratio, the distribution and dispersion of fillers in the polymer matrix, the interaction between fillers along with interfacial bonding and the manufacturing conditions [12,17]. The effect of filler loading on Young's modulus for all examined nanocomposites is described in Figure 5. Error bars represent the standard deviation of the respective results. The tensile modulus was determined as the slope of the stress-strain curve in the elastic region. A representative behavior for all examined systems is illustrated in Figure S3.

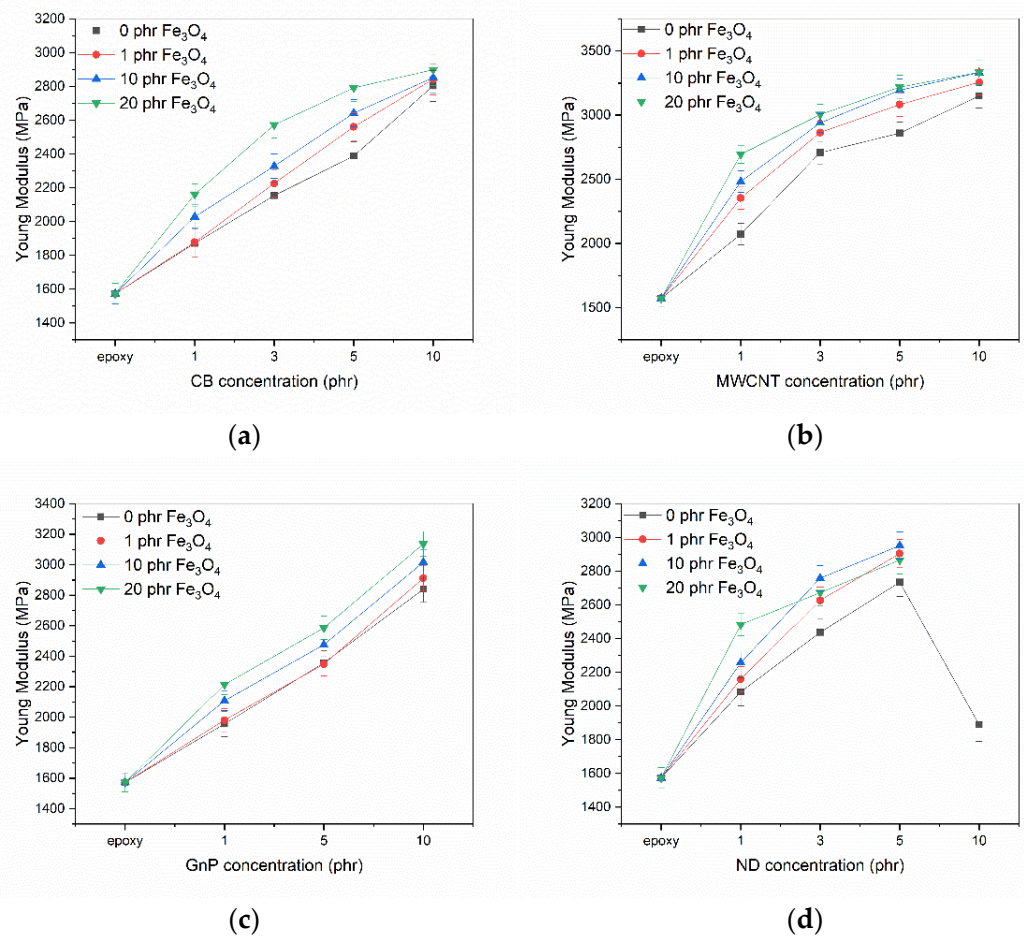


**Figure 5.** Young's modulus as a function of (a) CB; (b) MWCNT; (c) GnP; (d) ND concentration for all examined systems.

The addition of nanoparticles enhances the Young's modulus for all systems with the exception of the nanocomposites filled with nanodiamonds. The systematic increase in the tensile modulus values with filler loading denotes the ability of the nanoreinforcements to impart greater stiffness to the nanocomposites and is ascribed to the inherent stiffness and rigidity of the nanoparticles. The interfacial bonding provided by the strong interactions between the matrix and the nano-inclusions (as implied by the enhanced  $T_g$  values of the systems) effectively impacts the load transfer from the polymer matrix to nanofillers [16,24]. The addition of MWCNT and GnP leads to the largest modulus enhancement of all examined systems, an increase of more than 100% when compared with the neat epoxy, due to their aspect ratio and intrinsic stiffness. While the mechanical performance is largely dictated by the nanocarbon concentration, the addition of the iron oxide nanoparticles provides a further enhancement in the Young's modulus values. In the case of nanodiamonds filled nanocomposites, the maximum tensile modulus was achieved by the 5 phr ND/10 phr  $Fe_3O_4$  specimen. Further addition of  $Fe_3O_4$  nanoparticles limits the effective load transfer between the matrix and fillers, hence resulting in a reduction of Young's modulus.

The tensile strength of the nanocomposites, depicted in Figure 6, similar to the rest of the mechanical properties, is dictated by the local stress distribution around the reinforcements [25] that create a network which is able to bear the mechanical load. The tensile strength of the nanocomposites generally decreases with carbon concentration for all examined systems exhibiting lower values of strength than the polymer matrix. The nanocomposites with high aspect ratio fillers (MWCNT and GnP) retained higher values of tensile strength compared to the other systems. The addition of small amounts of magnetite nanoparticles (1 phr) leads to a small enhancement of the tensile strength for most systems. In fact, the specimens with 1 phr MWCNT/1 phr  $Fe_3O_4$  and 1 phr GnP/1 phr  $Fe_3O_4$  concentration exhibit marginally higher values of tensile strength in comparison with the matrix. Further addition of magnetite nanoparticles leads to a significant decrease in the tensile strength values because nanoparticles seem to act as stress raisers and/or stress concentration points. The latter is arguably a general problem in particulate-filled composites [2]. Overall, the hybrid GnP nanocomposites with 1 phr  $Fe_3O_4$  nanoparticles exhibit the optimum performance.

Elongation at break, also known as fracture strain, is the ratio between the length at breakage and the initial length of the sample and expresses the ability of the material to resist shape changes without crack development and propagation. The elongation at break as a function of filler content for all nanocomposites is presented in Figure 7. The addition of reinforcements leads to a substantial decrease of fracture strain values for all examined systems dropping from 3% for the neat epoxy to less than 1% for all systems with 20 phr magnetite concentration, irrespective of the type of carbon nanofiller. Diminishing of fracture strain is a clear indication of the reduction of ductility. It can be deduced that the reinforcing nanoparticles exert restrictions on chain mobility behaving as a type of "physical cross-linking points", as implied by the increase of  $T_g$  values, thus limiting the ability of the hybrid nanocomposites to easily adapt to the deformation because of the increase of their stiffness.

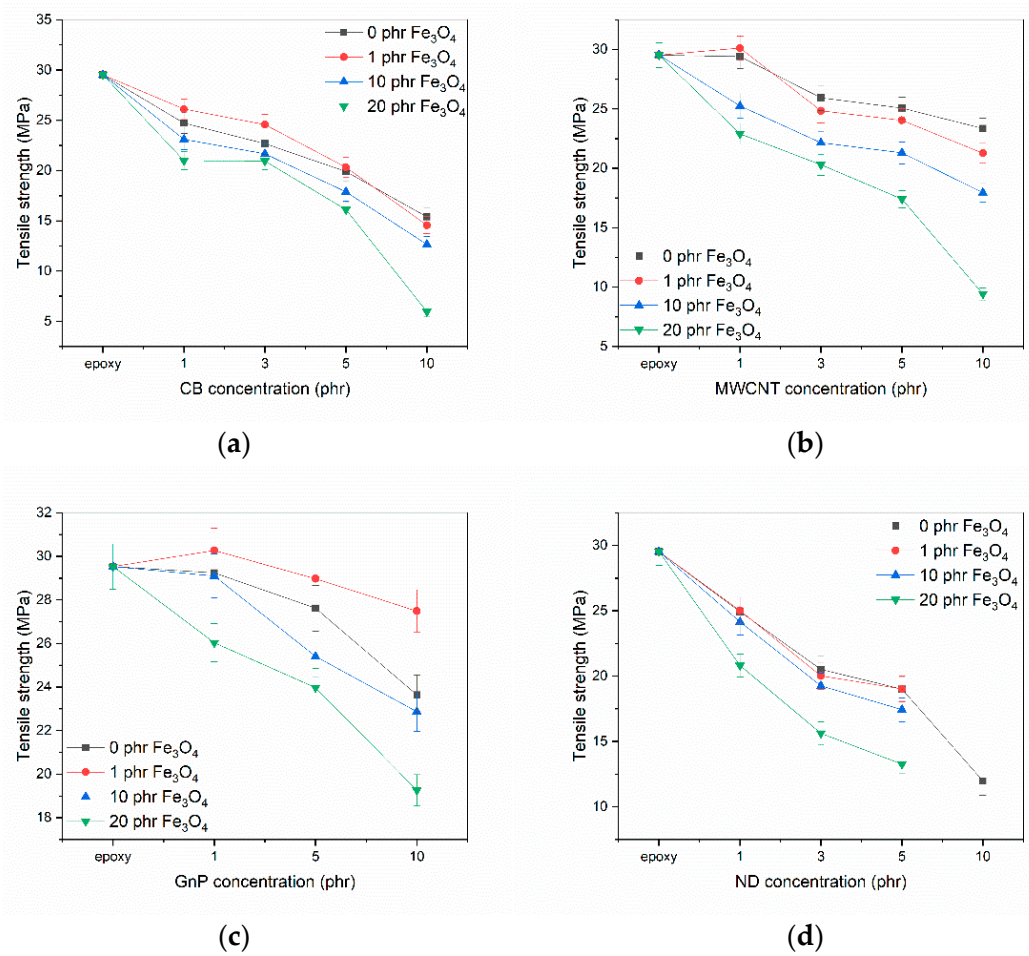


**Figure 6.** Tensile strength as a function of (a) CB; (b) MWCNT; (c) GnP; (d) ND concentration for all examined systems.

The estimation of the fracture toughness of the nanocomposites, depicted in Figure 8, was performed by integrating the stress strain curves and calculating the respective area. The incorporation of the nanoparticles to the polymer matrix, in general, leads to decreasing values of fracture toughness. The overall behavior of the systems is quite similar to the pattern observed in the figures illustrating the elongation at break as a function of filler content. The addition of 1 phr magnetite content does not have a detrimental effect in the nanocarbon filled composites, even exhibiting increasing fracture toughness in some cases. However, the excessive ceramic loading exerts a negative impact in the performance of all systems. The optimum performance was demonstrated by the 1 phr MWCNT/1 phr Fe<sub>3</sub>O<sub>4</sub> nanocomposite with a fracture toughness value of 65 kJ/m<sup>3</sup>.

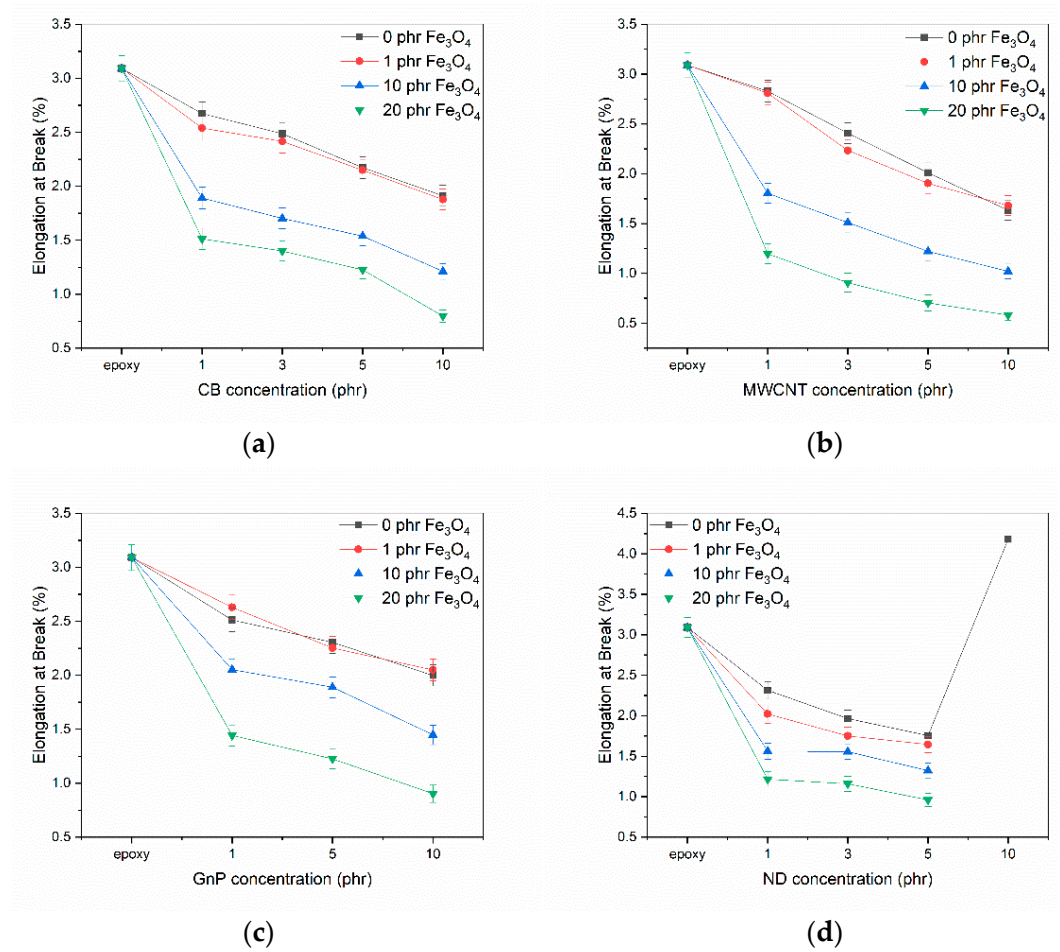


**Figure 7.** Elongation at break as a function of (a) CB; (b) MWCNT; (c) GnP; (d) ND concentration for all examined systems.

Overall, it can be noted that the reinforced systems do not display a clear/typical brittle performance with filler loading, since the diminishing fracture toughness and elongation at break values are not met with a respective increase in tensile strength but on the contrary, tensile strength values decrease with filler concentration, while Young’s modulus systematically increases. This behavior can be considered as a “stiffness strengthening” which ceases at higher mechanical loads, where the stress concentration at the nanoparticles, which are anchored at the macromolecular chains, leads to a failure at the interface.

Recalling that polymer matrix nanocomposites reinforced with carbonaceous and magnetic nanoparticles exhibit interesting electrical and magnetic properties [4–10], the assessment of their structural integrity and thermomechanical response introduces novel multitasking materials that could be employed in a variety of applications including electromagnetic interference (EMI), microwave electronic devices, capacitive energy storage and harvesting devices and as structural components with added functionalities in smart systems.

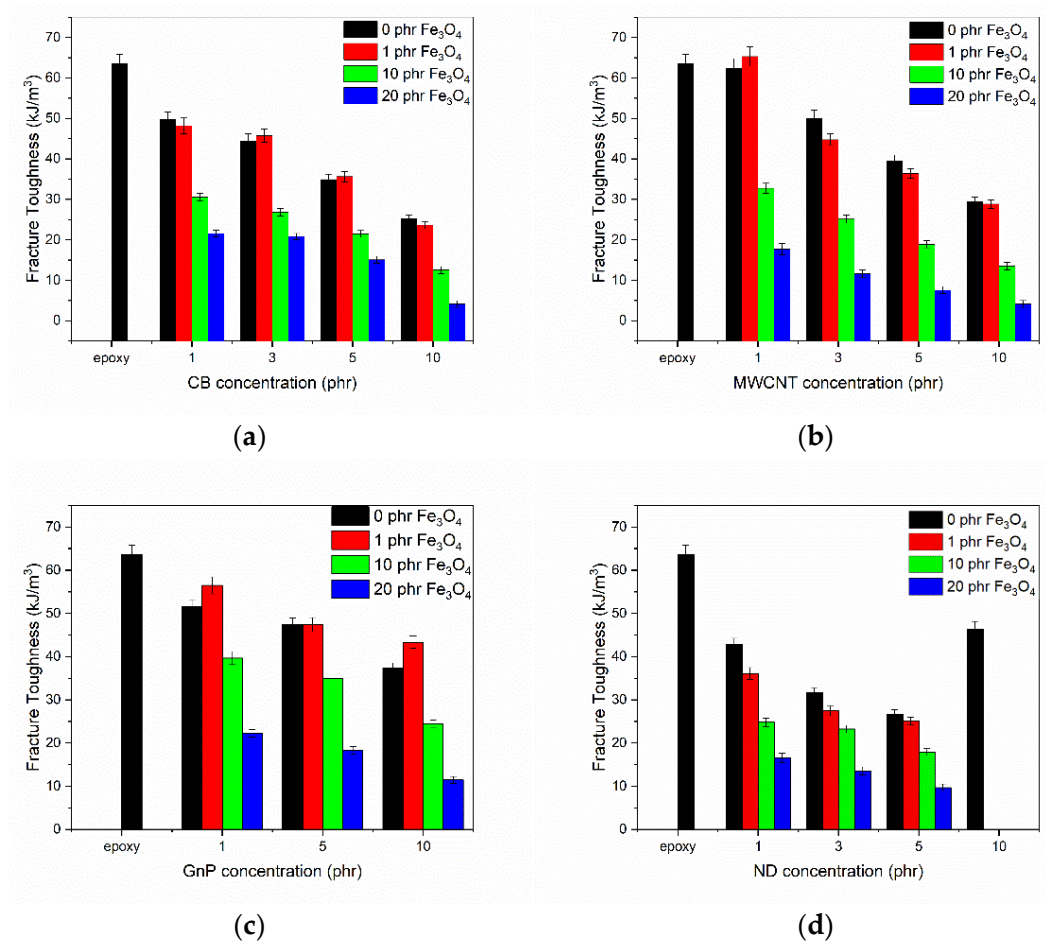


**Figure 8.** Fracture toughness as a function of (a) CB; (b) MWCNT; (c) GnP; (d) ND concentration for all examined systems.

#### 4. Conclusions

In this study, series of nanocomposites consisting of different carbonaceous (carbon black, MWCNTs, graphene nanoplatelets, nanodiamonds) and magnetite nanoparticles incorporated into a commercially available epoxy resin, were successfully fabricated varying the filler type and concentration. The hybrid nanocomposites exhibited higher glass transition temperature values than the unfilled epoxy showcasing the good adhesion of the reinforcing phase to the polymer matrix. The results from the static tensile tests and DMA demonstrated that the addition of both types of filler enhances the mechanical performance of the nanocomposites leading to increasing values of the tensile elastic modulus and the flexural storage modulus, respectively. The tensile strength of the nanocomposites generally decreases with filler concentration. The addition of small amounts of magnetite nanoparticles (1 phr), however, provided a small enhancement of the tensile strength for most systems. The examined systems presented a more brittle behavior since the addition of reinforcements leads to a substantial decrease of the fracture strain and fracture toughness values. The results demonstrate the potential development of novel multifunctional nanocomposite systems with adjustable properties and suitable thermomechanical performance, defining the corresponding ranges where these materials can operate safely at service.

**Supplementary Materials:** The following supporting information can be downloaded at: <https://www.mdpi.com/article/10.3390/applmech3020033/s1>, Figure S1: DSC thermograms for the nanocomposites with 10phr GnP content.; Figure S2: The variation of the (a) storage and (b) loss modulus as a function of temperature for the nanocomposites with 3phr MWCNT content.; Figure S3: Tensile strength vs. tensile strain for the systems with 3phr GnP content.

**Author Contributions:** S.G.S. and G.C.P. are responsible for the conceptualization and visualization; measurements, methodology, validation and data analysis were performed by S.G.S. and A.S.; writing and editing were performed by S.G.S., A.S., G.C.P.; project administration and supervision by G.C.P. All authors have read and agreed to the published version of the manuscript.

**Funding:** This research received no external funding.

**Data Availability Statement:** Data are included in the article.

**Acknowledgments:** The present research work was supported by the Hellenic Foundation for Research and Innovation (HFRI) and the General Secretariat for Research and Technology (GSRT) under the HFRI PhD Fellowship grant (GA. no.2327).

**Conflicts of Interest:** The authors declare no conflict of interest.

## References

1. Gu, H.; Ma, C.; Gu, J.; Guo, J.; Yan, X.; Huang, J.; Zhang, Q.; Guo, Z. An overview of multifunctional epoxy nanocomposites. *J. Mater. Chem. C* **2016**, *4*, 5890–5906. [[CrossRef](#)]
2. Saba, N.; Jawaid, M. A review on thermomechanical properties of polymers and fibers reinforced polymer composites. *J. Ind. Eng. Chem.* **2018**, *47*, 5475–5478. [[CrossRef](#)]
3. Hanemann, T.; Szabó, D.V. Polymer-Nanoparticle Composites: From Synthesis to Modern Applications. *Materials* **2010**, *3*, 3468–3517. [[CrossRef](#)]
4. Sanida, A.; Stavropoulos, S.G.; Speliotis, T.; Psarras, G.C. Evaluating the multifunctional performance of polymer matrix nanodielectrics incorporating magnetic nanoparticles: A comparative study. *Polymer* **2021**, *236*, 124311. [[CrossRef](#)]
5. Sanida, A.; Stavropoulos, S.G.; Speliotis, T.; Psarras, G.C. Probing the magnetoelectric response and energy efficiency in Fe<sub>3</sub>O<sub>4</sub>/epoxy nanocomposites. *Polym. Test* **2020**, *88*, 106560. [[CrossRef](#)]
6. Siwal, S.S.; Zhang, Q.; Devi, N.; Thakur, V.K. Carbon-Based Polymer Nanocomposite for High-Performance Energy Storage Applications. *Polymers* **2020**, *12*, 505. [[CrossRef](#)]
7. Martins, P.; Kolen'Ko, Y.V.; Rivas, J.; Lanceros-Mendez, S. Tailored Magnetic and Magnetoelectric Responses of Polymer-Based Composites. *ACS Appl. Mater. Interfaces* **2015**, *7*, 15017–15022. [[CrossRef](#)]
8. Stavropoulos, S.G.; Sanida, A.; Psarras, G.C. A comparative study on the electrical properties of different forms of carbon allotropes–epoxy nanocomposites. *Express Polym. Lett.* **2020**, *14*, 477–490. [[CrossRef](#)]
9. Gioti, S.; Sanida, A.; Mathioudakis, G.N.; Patsidis, A.C.; Speliotis, T.; Psarras, G.C. Multitasking Performance of Fe<sub>3</sub>O<sub>4</sub>/BaTiO<sub>3</sub>/Epoxy Resin Hybrid Nanocomposites. *Materials* **2022**, *15*, 1784. [[CrossRef](#)]
10. Stavropoulos, S.G.; Sanida, A.; Psarras, G.C. Carbon Allotropes/Epoxy Nanocomposites as Capacitive Energy Storage/Harvesting Systems. *Appl. Sci.* **2021**, *11*, 7059. [[CrossRef](#)]
11. Balguri, P.K.; Samuel, D.G.H.; Thumu, U. A review on mechanical properties of epoxy nanocomposites. *Mater. Today Proc.* **2021**, *44*, 346–355. [[CrossRef](#)]
12. Domun, N.; Hadavinia, H.; Zhang, T.; Sainsbury, T.; Liaghat, G.H.; Vahid, S. Improving the fracture toughness and the strength of epoxy using nanomaterials—A review of the current status. *Nanoscale* **2015**, *7*, 10294–10329. [[CrossRef](#)]
13. Frigione, M.; Lettieri, M. Recent Advances and Trends of Nanofilled/Nanostructured Epoxies. *Materials* **2020**, *13*, 3415. [[CrossRef](#)]
14. Paipetis, A.; Kostopoulos, V. (Eds.) *Carbon Nanotube Enhanced Aerospace Composite Materials; Solid Mechanics and Its Applications*; Springer: Dordrecht, The Netherlands, 2013; Volume 188, ISBN 978-94-007-4245-1.
15. Georgakilas, V.; Perman, J.A.; Tucek, J.; Zboril, R. Broad Family of Carbon Nanoallotropes: Classification, Chemistry, and Applications of Fullerenes, Carbon Dots, Nanotubes, Graphene, Nanodiamonds, and Combined Superstructures. *Chem. Rev.* **2015**, *115*, 4744–4822. [[CrossRef](#)]
16. Cha, J.; Jun, G.H.; Park, J.K.; Kim, J.C.; Ryu, H.J.; Hong, S.H. Improvement of modulus, strength and fracture toughness of CNT/Epoxy nanocomposites through the functionalization of carbon nanotubes. *Compos. Part B Eng.* **2017**, *129*, 169–179. [[CrossRef](#)]
17. Kausar, A. Nanocarbon and macrocarbonaceous filler–reinforced epoxy/polyamide: A review. *J. Thermoplast. Compos. Mater.* **2020**. [[CrossRef](#)]
18. Wang, X.; Tang, F.; Cao, Q.; Qi, X.; Pearson, M.; Li, M.; Pan, H.; Zhang, Z.; Lin, Z. Comparative Study of Three Carbon Additives: Carbon Nanotubes, Graphene, and Fullerene-C60, for Synthesizing Enhanced Polymer Nanocomposites. *Nanomaterials* **2020**, *10*, 838. [[CrossRef](#)]

19. Bychanok, D.; Kuzhir, P.; Maksimenko, S.; Bellucci, S.; Brosseau, C. Characterizing epoxy composites filled with carbonaceous nanoparticles from dc to microwave. *J. Appl. Phys.* **2013**, *113*, 124103. [[CrossRef](#)]
20. Cornell, R.M.; Schwertmann, U. *The Iron Oxides: Structure, Properties, Reactions, Occurrences and Uses*; Wiley-VCH Verlag GmbH & Co. KGaA: Weinheim, Germany, 2003; ISBN 3527302743.
21. Goldman, A. *Modern Ferrite Technology*, 2nd ed.; Springer: Pittsburgh, PA, USA, 2005; ISBN 9780387294131.
22. Jian, W.; Lau, D. Understanding the effect of functionalization in CNT-epoxy nanocomposite from molecular level. *Compos. Sci. Technol.* **2020**, *191*, 108076. [[CrossRef](#)]
23. Domun, N.; Paton, K.R.; Blackman, B.R.K.; Kaboglu, C.; Vahid, S.; Zhang, T.; Dear, J.P.; Kinloch, A.J.; Hadavinia, H. On the extent of fracture toughness transfer from 1D/2D nanomodified epoxy matrices to glass fibre composites. *J. Mater. Sci.* **2020**, *55*, 4717–4733. [[CrossRef](#)]
24. Menczel, J.D.; Prime, R.B. *Thermal Analysis of Polymers: Fundamentals and Applications*; Menczel, J.D., Prime, R.B., Eds.; John Wiley & Sons, Inc.: Hoboken, NJ, USA, 2009; ISBN 9780471769170.
25. Abraham, R.; Thomas, S.P.; Kuryan, S.; Isac, J.; Varughese, K.T.; Thomas, S. Mechanical properties of ceramic-polymer nanocomposites. *Express Polym. Lett.* **2009**, *3*, 177–189. [[CrossRef](#)]